

# Electropolymerization Kinetics of a Binary Mixture of Pyrrole and *O*-Aminobenzoic Acid and Characterization of the Obtained Polymer Films

S. M. Sayyah,<sup>1</sup> M. M. El-Rabiey,<sup>2</sup> S. S. Abd El-Rehim,<sup>3</sup> R. E. Azooz<sup>1</sup>

<sup>1</sup>Polymer Research Laboratory, Chemistry Department, Faculty of Science (Beni-Suef Branch), Cairo University, 62514 Beni-Suef, Egypt

<sup>2</sup>Chemistry Department, Faculty of Science, El-Fayoum University, El-Fayoum, Egypt

<sup>3</sup>Chemistry Department, Faculty of Science, Ain Shams University, Cairo, Egypt

Received 3 May 2007; accepted 29 November 2007

DOI 10.1002/app.28188

Published online 23 April 2008 in Wiley InterScience (www.interscience.wiley.com).

**ABSTRACT:** Poly (pyrrol-*co*-*o*-aminobenzoic acid) has been synthesized electrochemically from an aqueous acid medium. The initial rate of electrocopolymerization reaction on platinum electrode is small and the rate law is: Rate =  $K_2 [D]^{1.02} [HCl]^{1.44} [M]^{2.00}$ . The apparent activation energy ( $E_a$ ) is found to be 90.11 kJ mol<sup>-1</sup>. The polymer films obtained have been characterized by cyclic voltammetry, X-ray diffraction, elemental analysis, thermogravi-

metric analysis, scanning electron microscopy, <sup>1</sup>H NMR, and IR-spectroscopy. The mechanism of the electrochemical polymerization reaction has been discussed. The monomer reactivity ratios ( $r_1$  and  $r_2$ ) were calculated. © 2008 Wiley Periodicals, Inc. *J Appl Polym Sci* 109: 1643–1653, 2008

**Key words:** kinetics (polym.); structure; TGA; morphology; X-ray

## INTRODUCTION

Many studies have been devoted to the (potential) applications of conducting polymers especially electroactive polymers deposited electrochemically on electrode surfaces because of the many possible applications of the polymers themselves as well as the modified electrode surfaces in; batteries,<sup>1–7</sup> electrochromic devices,<sup>2,8–10</sup> microelectronic devices,<sup>11</sup> optoelectronic,<sup>12</sup> display devices,<sup>13</sup> chemically modified electrodes,<sup>14</sup> sensors,<sup>15,16</sup> electrochemical chromatography,<sup>17</sup> metallization,<sup>18</sup> and as corrosion inhibitors to protect semiconductors and metals.<sup>18–28</sup>

Polymers such as poly(thiophene)s, poly(pyrrole)s, poly(aniline)s, etc. were prepared. Among all these polymers particular interest has been paid to poly(aniline) (PANI) and poly(pyrrole).

Owing to the ease of its preparation, outstanding stability, and good electrical conductivity,<sup>29</sup> PANI is one of the most common electroactive polymers that have found many applications. These applications are limited by the insolubility of its protonated state due to the stiffness of its backbone, difficulty of proceeding by conventional methods. One of the methods which is used to overcome this problem is the polymerization of different substituted aniline deriv-

atives.<sup>19,25</sup> The obtained polymers have higher solubility and thus improved solution processibility.<sup>30</sup>

*O*-aminobenzoic acid (OABA) is considered as an ortho-carboxylic substituted aromatic ring of aniline. It was polymerized chemically.<sup>31–33</sup> Also it was polymerized electrochemically by potential sweep in H<sub>2</sub>SO<sub>4</sub> solution on glassy carbon electrode,<sup>34</sup> the rate of electropolymerization increased by adding aniline which form a copolymer, and in aqueous HCl solution on platinum electrode by Sayyah et al.<sup>35</sup> the kinetics of the electropolymerization process were found. The obtained polymer (POABA) is of interest as a soluble derivative of PANI, soluble in polar solvent like *N*-methylpyrrolidone in a neutral state, and soluble even in alcohols and water in the carboxylic ion state.<sup>33</sup> Furthermore, poly(*o*-aminobenzoic acid) can have a ring structure due to intermolecular hydrogen bond, which is similar to the structure of self doped sulfonated PANI.<sup>36</sup> The introduction of acidic group influence the acidity constant of the amine group and appears to offer advantages at less acidic pH values, since conductivity does not fall dramatically with increase pH as happens with PANI.<sup>32,33</sup>

In the series of conducting polymers, considerable attention was drawn to the pyrrole family of polymers prepared by electrochemical oxidation such as polypyrrole, poly(*N*-methyl pyrrole) and their copolymers for their applications in solid state devices.<sup>37</sup> Several investigations have been performed to observe the effect of various parameters such as

Correspondence to: S. M. Sayyah (smsayyah@hotmail.com).

solvent, electrolyte and temperature on the mechanical strength, stability, and conductivity.<sup>38–45</sup> Sayyah et al.<sup>46</sup> studied the electrochemical oxidative polymerization of pyrrole on platinum electrode in acid medium and the kinetics of the electropolymerization process.

In this study, we intend to investigate the kinetics, optimum conditions, and mechanism of the electrochemical copolymerization of a binary mixture of pyrrole and *o*-aminobenzoic acid in aqueous HCl solution on platinum electrode. Also, the characterization of the obtained copolymer films by <sup>1</sup>H NMR, IR, elemental analysis, thermogravimetric analysis (TGA), and cyclic voltammetry was performed.

## EXPERIMENTAL

### Materials

*O*-aminobenzoic acid (Fluka, Switzerland), hydrochloric acid solution (Riedel-de Haën, Germany), and dimethylformamide were provided by El-Naser pharmaceutical Chemical Company (Egypt), pyrrole, and anhydrous sodium sulfate were provided by Merck (Darmstadt, Germany). All solutions are freshly prepared using double distilled water.

### Cell and electrodes

The experimental set up used consisted of a rectangular Perspex cell provided with two platinum foil parallel electrodes [dimensions: 1 cm height × 0.5 cm width] as described previously.<sup>46–49</sup> The polymerization current was supplied by a dc power supply [Thurby ~ Thandar PL 330]. Before each run, the platinum electrode (anode) was cleaned, washed with distilled water, rinsed with ethanol, dried, and weighed. The experiments were done at the required temperature ± 1°C using a circular water thermostat. At the end of the experiment, the anode was withdrawn, washed with distilled water, dried, and weighed using a 4504 MP8 Sartorius ultramicrobalance (10<sup>-7</sup> gm precision).

### Electropolymerization reaction

Anodic oxidative electrocopolymerization of a binary mixture of *o*-aminobenzoic acid and pyrrole was carried out in aqueous solutions containing monomer (concentration range between 0.01 and 0.13M) using 0.1M Na<sub>2</sub>SO<sub>4</sub> as the supporting electrolyte and the current densities were investigated in the range between 2 and 10 mA cm<sup>-2</sup>. Electrocopolymerization was carried out in hydrochloric acid solution (concentration range between 0.2 and 1.0M) at different temperatures in the range between 294 and 323 K.

### Cyclic voltammetry measurements

A standard three-electrode cell was used in the cyclic voltammetry measurements with a saturated calomel electrode as the standard reference electrode. The auxiliary electrode was a platinum wire. The dimensions of the platinum working electrode were 1 × 0.5 × 0.05 cm<sup>3</sup>. Before each run, the working electrode was cleaned as mentioned above.

The electrochemical experiments were performed using an EG and G Potentiostat/Galvanostat Model 273 supplied by EG and G Princeton Applied Research. The I-E curves were recorded by computer software from the same company (Model 352 and 270/250).

### Infrared, <sup>1</sup>H NMR spectroscopy, thermogravimetric, and elemental analysis

Infrared measurements were carried out using a Shimadzu Ftir-430 Jasco spectrophotometer.

<sup>1</sup>H NMR measurements were carried out using a Varian EM 360 L, 60 MHz NMR spectrometer. NMR signals of the obtained polymer were recorded using dimethyl sulfoxide as a solvent and tetramethyl silane as internal reference.

Thermogravimetric analyses of the obtained polymers were performed using a Shimadzu DT-30 thermal analyzer. The weight loss was measured from ambient temperature up to 600°C, at the rate of 10°C/min to determine the degradation rate of the polymer.

Elemental analysis was carried out in the microanalytical center at Cairo University by oxygen flask combustion and dosimat E415 titrator (Switzerland).

### Scanning electron microscopy and X-ray diffraction

Scanning electron microscopic analysis was carried out for the polymer film adhered on the platinum electrode using a JSM-T20 scanning electron microscope, (JEOL, Tokyo, Japan).

The X-ray diffraction analysis (XRD) was carried out by X-ray diffractometer (Philips 1976 Model 1390, Netherlands) which operated for the polymer film adhered on the platinum electrode under the following conditions that were kept constant for all the analysis processes: X-ray tube: Cu; Scan speed: 8 deg/min; Current: 30 mA; Voltage : 40 kV; Preset time: 10 s.

### Molecular weight determination

Molecular weights of the obtained polymer samples were determined using HPLC system (GPC mode) instrument model HP-1100, Isocratic pump (1 mL/

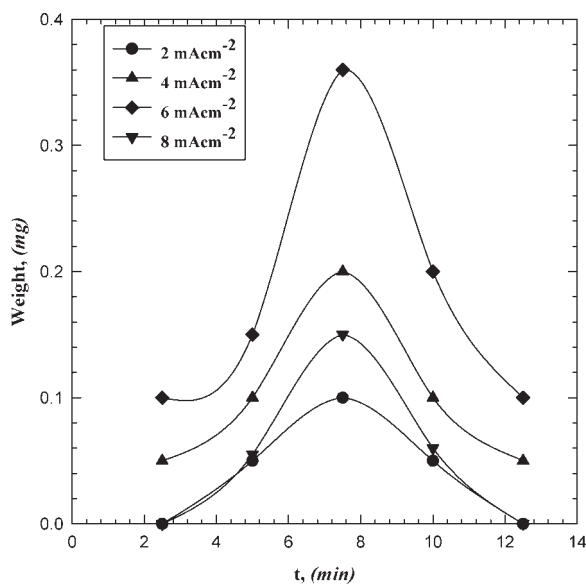


**Figure 1** Yield-time curve for the effect of duration time on the anodic copolymerization of a mixture of pyrrole and *o*-aminobenzoic acid from solution containing 0.05M monomer, 1.0M HCl, and 0.1M Na<sub>2</sub>SO<sub>4</sub> at 304 K.

min, solvent THF), column type 2 pl Gel 10 mj mixed bed 300 × 7.5 mm<sup>2</sup> and gaured at 40°C.

## RESULTS AND DISCUSSION

### Anodic oxidative electrocopolymerization

#### Effect of duration time

Anodic oxidative electrocopolymerization of a binary mixture of *o*-aminobenzoic acid and pyrrole was studied under the influence of different plating and operating parameters. The effect of duration time on the weight of the obtained polymer films was stud-

ied with different current density values. The data reveal that the weight of the obtained polymer increases with increase of duration time up to 7.5 min, after which it began to decrease as a result of degradation and the solubility of the polymer film from the platinum surface in the case of all investigated values of the current density. The data are graphically represented in Figure 1.

#### Effect of current density

The effect of the applied current density on the anodic oxidative electrocopolymerization reaction of a binary mixture of *o*-aminobenzoic acid and pyrrole was studied at 7.5 min (optimum duration time) using 0.09M monomer concentration (1:1M ratio), 0.1M Na<sub>2</sub>SO<sub>4</sub> in aqueous solution and 1.0M HCl at 304 K. All the above-mentioned parameters were kept constant while the current density was varied. The data reveal that, as the applied current density value increases, the weight of the obtained copolymer film increases up to 6 mA cm<sup>-2</sup> and then tends to decrease as a result of side reactions involving the evolution of chlorine and oxygen gas especially at high current densities. Each value of the applied current density was studied over different time intervals and the yield-time curves are graphically represented in Figure 2(A), from which the initial rate ( $R_i$ ) of the electrocopolymerization was determined. The exponent of the electrocopolymerization reaction with respect to the current density was determined from the slope of the straight line obtained from the double logarithmic relationship between current density values and initial rates, which is presented in Figure 2(B). The exponent is found to be 1.02, which means that, the reaction order is a first order with respect to the current density.

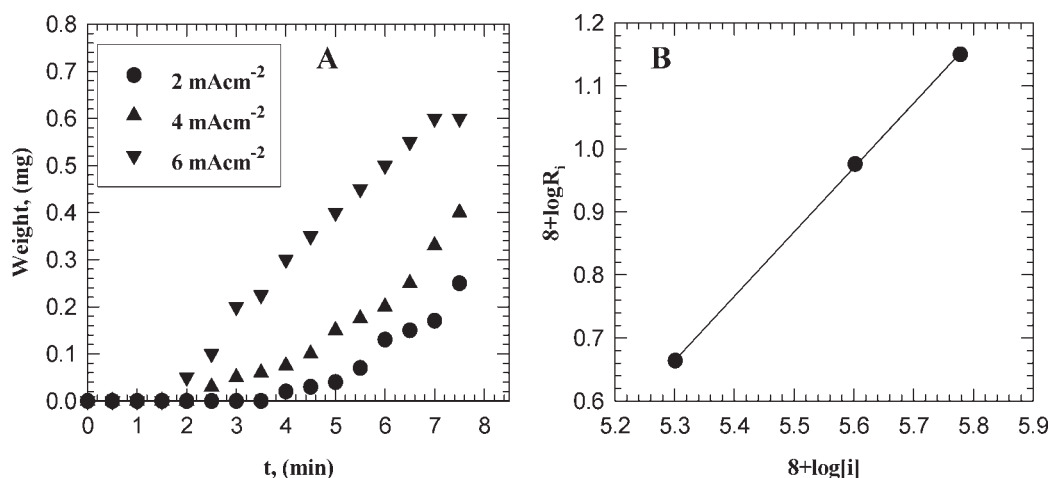


**Figure 2** (A) Yield-time curve for the effect of current densities. (B) Double-logarithmic plot of initial rate of electrocopolymerization versus different current density values.

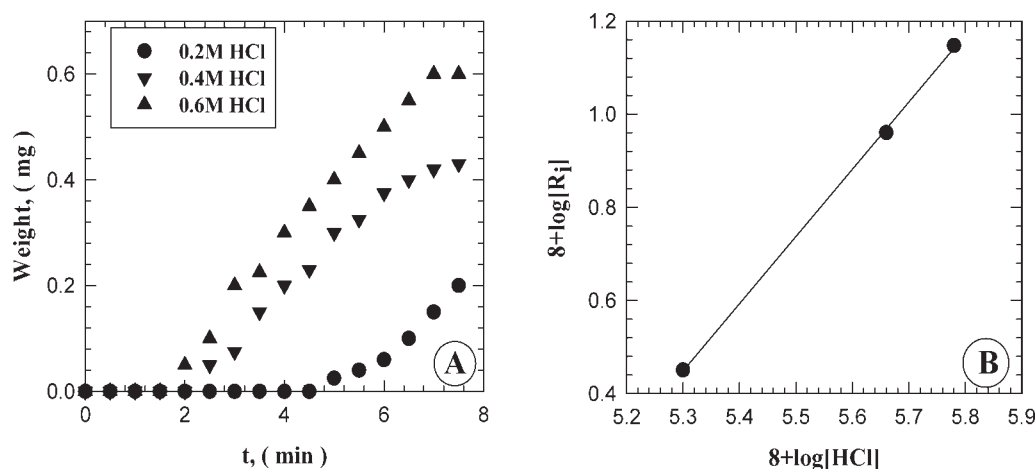


**Figure 3** (A) Yield-time curve for the effect of HCl concentrations. (B) Double-logarithmic plot of initial rate of electrocopolymerization versus different HCl concentrations.

#### Effect of HCl concentration

Anodic oxidative electrocopolymerization was carried out using 0.09M monomer concentration (1 : 1M ratio), 0.1M  $\text{Na}_2\text{SO}_4$  in aqueous solution, current density =  $6 \text{ mA cm}^{-2}$ , duration time (7.5 min) at 304 K, which were kept constant but the hydrochloric acid concentration was varied in the range between 0.2 and 1.0M. The weight of the obtained copolymer film in each experiment was determined. The obtained data shows that, the maximum weight is obtained when 0.6M HCl concentration is used. The effect of HCl concentrations on the electrocopolymerization rate is carried out in the concentration range between 0.2 and 0.6M. The weight of the deposited copolymer film on the platinum electrode in each experiment was determined and graphically represented in Figure 3(A). The initial rate ( $R_i$ ) of the electrocopolymerization reaction was calculated and the double logarithmic plot of the initial rate versus HCl concentrations is represented in Figure 3(B). A

straight line is obtained which has a slope equal to 1.44.

#### Effect of monomer concentration

The anodic oxidative electrocopolymerization reaction was carried out by keeping the following conditions constant at 0.6M HCl, current density =  $6 \text{ mA cm}^{-2}$ ,  $\text{Na}_2\text{SO}_4$  (0.1M), duration time (7.5 min), and temperature at 304 K, but the monomer concentrations were varied in the range between 0.01 and 0.13M (1 : 1M ratio). The weight of the obtained copolymer film in each case was determined. From the obtained data, it is noticed that, the maximum weight of the copolymer film is obtained when 0.09M monomers mixture concentration (1 : 1M ratio) is used. It is also noticed that, the weight of the copolymer film decreases at higher concentrations than 0.09M of the monomer mixture. The electrocopolymerization of a mixture of *o*-aminobenzoic acid and pyrrole is performed using different mono-

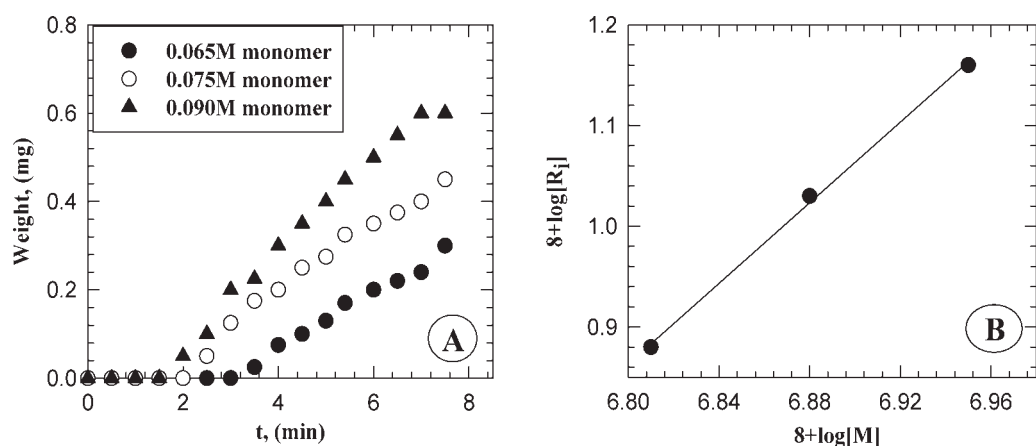


**Figure 4** (A) Yield-time curve for the effect of monomer concentrations. (B) Double-logarithmic plot of initial rate of electrocopolymerization versus different monomer concentrations.



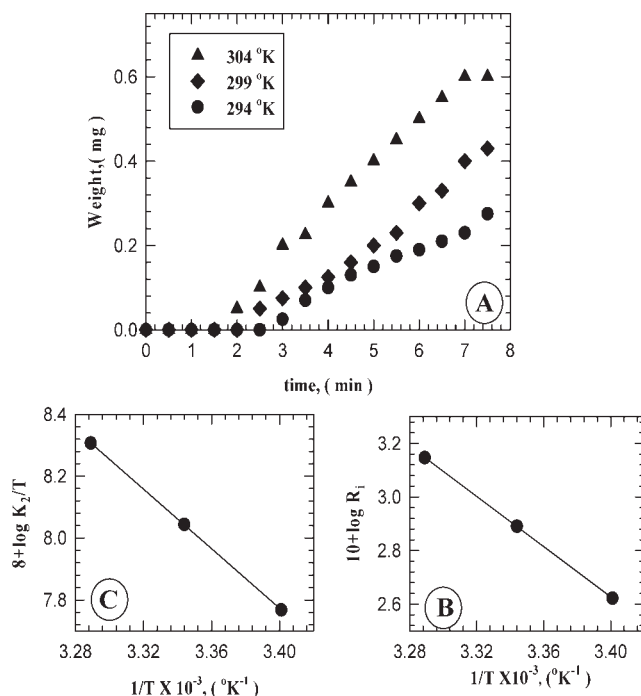


**Figure 5** (A) Yield-time curve for the effect of temperature. (B) Arrhenius plot for the electrocopolymerization. (C) Eyring equation plot for the electrocopolymerization.

mer concentrations in the range between 0.065 and 0.09M (1 : 1M ratio) at different time intervals. The data are recorded and graphically represented in Figure 4(A). The initial rate ( $R_i$ ) of the electrocopolymerization was calculated and the double logarithmic plot of the initial rate of the electrocopolymerization versus the monomer concentration is represented in Figure 4(B). This relationship gives a straight line with a slope equal to 2.0, which means that the order of the electrocopolymerization reaction is a second order reaction with respect to the monomer concentration.

#### Effect of temperature

Anodic oxidative electrocopolymerization of a binary mixture of *o*-aminobenzoic acid and pyrrole was carried out under the following constant conditions: 0.6M HCl, 0.09M monomer (1 : 1M ratio), 0.1M  $\text{Na}_2\text{SO}_4$ , 6  $\text{mA cm}^{-2}$ , and the duration time 7.5 min but the reaction was carried out at different temperatures in the range between 294 and 323 K. The weight of the obtained copolymer film was recorded at each investigated temperature. The data shows that, the maximum weight of the copolymer film was recorded at 304 K. It is noticed during the experiments that, at higher temperatures than 304 K, some copolymers are formed in the solution near the anode which do not adheres to the electrode, which means that, at temperatures higher than 304 K, the adhesion of the film to the electrode surface

decreases. The electrocopolymerization of a binary mixture of *o*-aminobenzoic acid and pyrrole was carried out at different temperatures 294, 299, 298, and 304 K for different time intervals. At each temperature the weight of the formed copolymer at the anode at different time intervals was determined and the yield-time curves are represented in Figure 5(A). The initial rate ( $R_i$ ) of the electrocopolymerization reaction was calculated at each investigated temperature and the logarithm of the initial rate was plotted versus  $1/T$  [cf. Fig. 5(B)], which gives a straight line with a slope equal to  $-4.69$ . By applying Arrhenius equation,<sup>35,46-49</sup> the apparent activation energy was calculated and it is found to be  $87.75 \text{ kJ mol}^{-1}$ .

#### Calculation of thermodynamic parameters

The enthalpy  $\Delta H^*$  and entropy  $\Delta S^*$  of activation for the electrocopolymerization reaction can be calculated from the  $k_2$  values of eq. (1). The values of  $k_2$  at different temperatures were calculated and the enthalpy ( $\Delta H^*$ ) and entropy ( $\Delta S^*$ ) of the activation associated with  $k_2$  were calculated using the Eyring equation [eq. (2)].

$$\text{Reaction rate} = k_2[\text{HCl}]^{1.44}[\text{current density}]^{1.02} \times [\text{monomer}]^{2.00} \quad (1)$$

$$k_2 = RT/Nh e^{\Delta S^*/R} e^{\Delta H^*/RT} \quad (2)$$

where  $k_2$  is the rate constant,  $R$  is the universal gas constant,  $N$  is Avogadro's number, and  $h$  is the Planck's constant. By plotting  $\log k_2/T$  versus  $1/T$  [cf. Fig. 5(C)] we obtained a linear relationship with a slope of  $-\Delta H^*/2.303R$  and intercept of  $\log \{(R/Nh) + \Delta S^*/2.303R\}$ . From the slope and intercept,<sup>35,46-49</sup> the values of  $\Delta H^*$  and  $\Delta S^*$  were found to be  $90.11 \text{ kJ mol}^{-1}$  and  $+111.45 \text{ JK mol}^{-1}$ , respectively.

#### Elemental analysis and Spectroscopic analysis

##### Elemental analysis

Elemental analytical data are given in Table I, which are in good agreement with those calculated for the suggested structure represented in Scheme 2.

##### Thermogravimetric analysis

TGA for the electrochemically prepared P(OABA-co-Py) copolymer sample has been investigated and the thermal degradation steps are represented in Table II and described as follows:

**TABLE I**  
Elemental Analysis of the Prepared Copolymer

	%C	%H	%N	%Cl
Calcd.	51.8	04.76	10.09	10.24
Found	50.68	04.90	09.80	10.23

**TABLE II**  
**Thermogravimetric Data of the Prepared P(OABA-co-Py)**

Temperature range (°C)	Weight loss (%)		The removed molecule
	Calculated	Found	
25–111	5.31	6.09	2H <sub>2</sub> O
111–284	14.78	14.30	2H <sub>2</sub> O + 3HCl
284–423	16.52	15.04	3 COOH + H <sub>2</sub> O
423–600	47.83	48.50	H <sub>2</sub> O + 3 pyrrole moiety + 3 benzenoid moiety
>600	–	16.00	Carbon + Na <sub>2</sub> SO <sub>4</sub>

*First stage.* It includes the loss of three molecules of water. In the temperature range between 26 and 111°C, the weight of loss for this step is found to be 6.09%, which is in a good agreement with the calculated one (5.31%).

*Second stage.* In the temperature range between 111 and 284°C, the weight loss was found to be 14.78%, which is attributed to the loss of two water molecules and three HCl molecules. The calculated weight loss in this case is equal to 14.03%.

*Third stage.* In the temperature range between 284 and 423°C, the weight loss is found to be 16.52%, which may be due to the lost of three COOH groups and one water molecule. The calculated weight loss of this stage is equal to 15.04%.

*Fourth stage.* In the temperature range between 423 and 600°C, the weight loss is found to be 47.83%, which may be due to the lost of three pyrrole moiety, one water molecule and three benzenoid moiety. The calculated weight loss of this stage is equal to 48.50%.

*Last stage.* Above 600°C, a residual material (16%) is remained.

The thermal stability of the copolymer P(OABA-co-Py) and the previously investigated two homopolymers POABA<sup>35</sup> and Ppy<sup>35</sup> have the following order:



#### <sup>1</sup>H NMR spectroscopic analysis

The <sup>1</sup>H NMR spectrum of the prepared copolymer P(OABA-co-Py) in comparison with those of the two homopolymers poly (OABA) and (Ppy) —the assignments are taken from<sup>50</sup>—give the following characteristic signals:

1. The two singlet signals at  $\delta = 2.5$  ppm and  $\delta = 3.5$  ppm, which are attributed to solvent protons.
2. The benzene ring protons appear as a multiplet signal in the region from  $\delta = 7 \leftrightarrow 8$  ppm in case of poly (OABA), and in case of the copolymer, but the singlet signal appears in the case of

(Ppy) at  $\delta = 7.67$  could be attributed to NH protons of pyrrole ring.

3. The singlet signal appearing at  $\delta = 11$  ppm in case of (POABA), at  $\delta = 8.8$  ppm in case of (Ppy), and at  $\delta = 8.7$  ppm in case of the copolymer are due to the OH end group protons.

#### IR spectroscopic analysis

The IR spectrum of the prepared copolymer (poly (*o*-aminobenzoic acid-co-pyrrole)) in comparison with those of the two homopolymers, poly (*o*-aminobenzoic acid) p(OABA),<sup>35</sup> and poly (pyrrole) (Ppy)<sup>46</sup> shows that the medium absorption band appearing at 595 cm<sup>-1</sup>, which may be attribute to NH deformation in pyrrole ring in case of the (Ppy), appears as a weak absorption band in case of copolymer at 612 cm<sup>-1</sup>. The medium absorption band appearing at 671 cm<sup>-1</sup>, which may be attributed to the stretching vibration of NH in pyrrole ring in case of the (Ppy), appears as a weak absorption band in case of copolymer at 674 cm<sup>-1</sup>. The medium absorption bands appearing at 757 and 759 cm<sup>-1</sup>, which may be attribute to the CH deformation of (1,2) or (1,4) disubstituted benzene ring in case of the poly (OABA), appears as a medium absorption band in case of copolymer at 789 cm<sup>-1</sup>. The weak band appearing at 1022 cm<sup>-1</sup> and a medium band appearing at 1044 cm<sup>-1</sup>, could be attributed to the C—C stretching vibration in case of poly(OABA), appear at 1021 cm<sup>-1</sup> (broad band) in case of Ppy and appear as a sharp band at 1042 cm<sup>-1</sup> in case of copolymer. The broad band appearing at 1251 cm<sup>-1</sup>, could be attributed to the C-O stretching vibrations, in case of poly (OABA) appears at 1201 cm<sup>-1</sup> as broad band in case of copolymer. The strong absorption band, which appearing at 1402 cm<sup>-1</sup> in case of poly OABA, appears as two weak bands and a medium one at 1324, 1351, and 1405 cm<sup>-1</sup>, respectively, in case of Ppy, appearing as two weak bands at 1351 and 1373 cm<sup>-1</sup> in case of copolymer, could be due to C—N stretching vibrations. The medium absorption band appearing at 1465 cm<sup>-1</sup>, may be assigned to the symmetric stretching vibration of (C=N) group in quinoide structure, in case of (Ppy) appear at 1464 cm<sup>-1</sup> as strong band in case of poly OABA and as a medium absorption band in case of the copolymer. The strong absorption band appearing at 1461 cm<sup>-1</sup> (in case of copolymer), appearing as weak absorption band at 1506 cm<sup>-1</sup> (in case of poly OABA) are ascribed to the scissoring vibrations for NH. The absorption bands appearing at 1627 cm<sup>-1</sup> (broad) and at 1661 cm<sup>-1</sup> (medium) in case of Ppy, appearing as a broad band at 1652 cm<sup>-1</sup> in case of poly OABA, appears as a weak band at 1649 cm<sup>-1</sup> in case of the copolymer, could be attributed to the C=C stretching vibration in benzene ring or five mem-

TABLE III  
Infrared Absorption Bands of the IR Spectrum of POABA, PPy, and P(OABA-co-Py) Samples

Names			
Wave number (cm <sup>-1</sup> )			
POAB <sup>35</sup>	PPy <sup>46</sup>	Copolymer	Assignments <sup>50</sup>
–	595 (m)	612 (w)	NH deformation in pyrrole ring
–	671 (m)	674 (w)	Stretching vibration of NH in pyrrole ring
757 (m), 759 (m)	–	789 (m)	CH deformation of (1,2) or (1,4) di substituted benzene ring
1022 (w), 1044 (m)	1021 (b)	1042 (s)	C–C stretching vibrations
1251 (b)	–	1201 (b)	C–O stretching vibrations
1402 (s)	1324 (w), 1351 (w), 1405 (m)	1351 (w), 1373 (w)	C–N stretching vibrations
1464 (s)	1465 (m)	1461 (m)	C=N stretching vibration in quinoide structure
1506 (w)	–	1556 (s)	NH scissoring vibrations
1652 (b)	1627 (b), 1661 (m)	1649 (w)	Stretching vibration for C=C in benzene ring or in five member ring
1702 (b)	–	1701 (w)	Stretching vibrations of C=O in carboxylic group
2925 (s)	2950 (w)	2925 (m)	Stretching vibration for protonated primary aromatic amine
3425 (b)	3410 (b)	3425 (b)	Symmetric stretching vibration of NH in pyrrole ring or symmetric stretching of OH (hydrogen bonded) in carboxylic acid

s, strong; w, weak; b, broad; m, medium.

bered ring of pyrrole. The other IR absorption bands and their assignments are tabulated in Table III.

#### Molecular weight determinations

The molecular weight data obtained by GPC analysis was found to be as follows:

$M_w = 8.06 \times 10^5$ ,  $M_n = 7.60 \times 10^5$ ,  $M_v \times 10^5$ , and the polydispersity (Pd) = 1.06.

#### Copolymer structure and the mechanism

The monomer reactivity ratios of the copolymerization system ( $r_1$  and  $r_2$ ) involving pyrrole and *o*-aminobenzoic acid were determined on the basis of comonomer composition—copolymer composition relationship. The monomer reactivity ratios were calculated according to Fineman-Ross method<sup>51</sup> using <sup>1</sup>H NMR spectroscopy as a quantitative analytical tool.

#### Fineman-Ross method

The oxidative electrocopolymerization was carried out as described previously under point 2.3, but with different molar ratios of the two monomers.

The two monomers are incorporated into the copolymer chain depending on their relative concentrations and reactivities. The composition of the copolymer was quantitatively determined by <sup>1</sup>H NMR analysis of the copolymer samples and the monomer reactivity ratios  $r_1$  and  $r_2$  of this copolymer was cal-

culated from Fineman-Ross equation [eq. (3)] and represented in Figure 6.

$$F/f(f-1) = r_1(F^2/f) - r_2 \quad (3)$$

where,  $F = M_1/M_2$  (molar ratio for monomer feed composition) and  $f = m_1/m_2$  (molar ratio for copolymer composition).

The slope is equal to  $r_1$  and the intercept is equal to  $-r_2$ . From the figure, it was found that  $r_1 = 1.58$

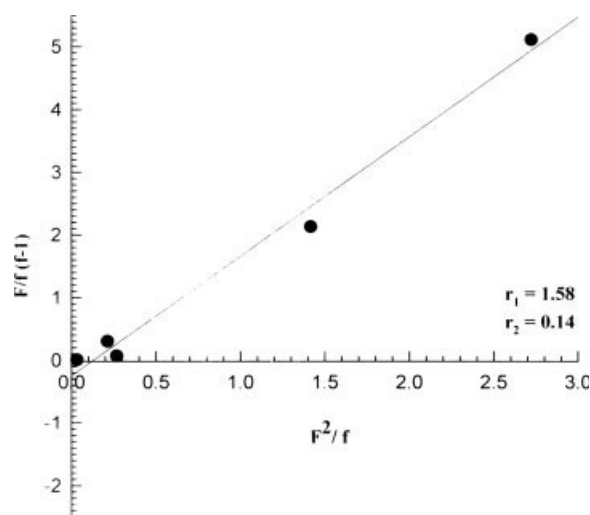
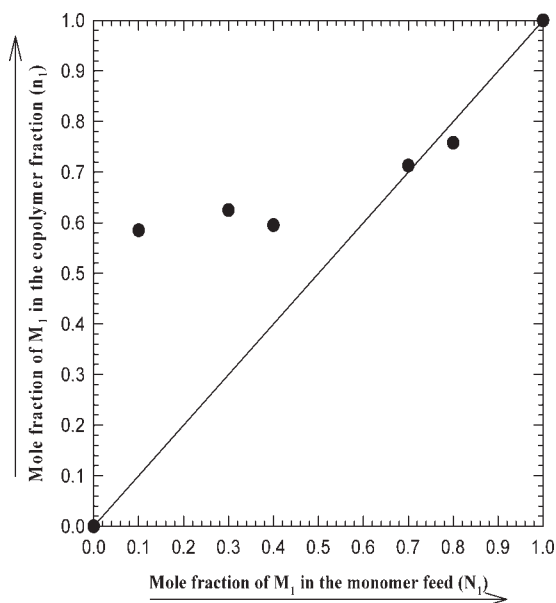


Figure 6 Fineman-Ross plot for the determination of monomer reactivity ratio of pyrrole and *o*-aminobenzoic acid in aqueous HCl solution copolymerized by electrochemical method on Pt-electrode.



**Figure 7** Composition curve for the electrocopolymerization between pyrrole ( $M_1$ ) and *o*-aminobenzoic acid ( $M_2$ ) in aqueous HCl solution on Pt electrode.

and  $r_2 = 0.14$ . From the data, the value of  $r_1$  is more than one and  $r_2$  is less than one. In this case the propagation reaction type 11 and 21 will be preferred than the type 12 and 22, hence the probability of  $M_1$  (Py) entering into the copolymer chain is higher when compared with  $M_2$  (OABA), therefore the formed copolymer will be richer in  $M_1$ .

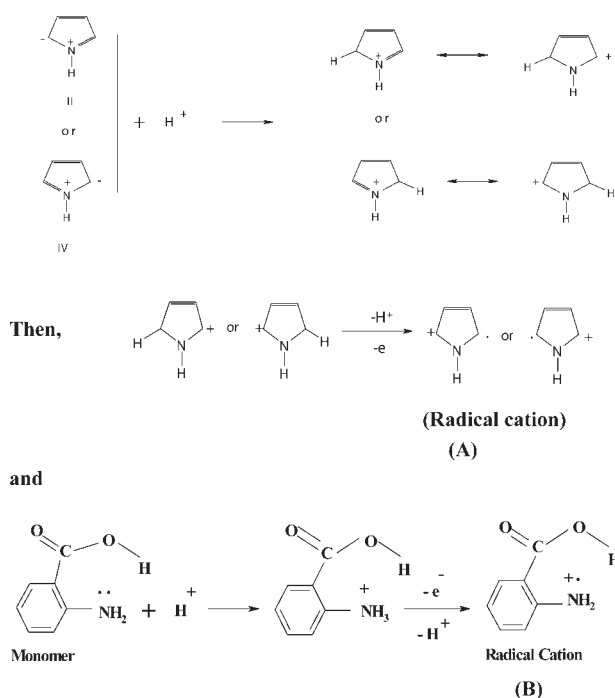
The copolymer composition data for the investigated system were calculated and the relation between the mole fraction of  $M_1$  in the formed copolymer ( $n_1$ ) and the mole fraction of  $M_1$  in the monomer feed ( $N_1$ ) and are plotted in Figure 7. The diagonal line represents the case that both monomers have identical reactivity. The values of  $n_1$  for the copolymers are above the diagonal line up to ( $n_1 = 0.7$ ) then tends to be down the diagonal line indicating that the copolymers consist of a higher fraction of Py units than that of OABA units and that the Py is much more reactive than OABA up to ( $n_1 = 0.7$ ). After that the reactivity of OABA is more than that of Py. From the above data, it is clear that the copolymer structure is a block copolymer structure; therefore the copolymerization mechanism can be represented as shown in Schemes 1 and 2.

### Cyclic voltammetric characterization

Cyclic voltammograms of the two separate monomers *o*-aminobenzoic acid and pyrrole and the binary mixture of the two monomers with molar ratio 1 : 1 in aqueous acid medium in the presence of 0.6M HCl and 0.1M  $\text{Na}_2\text{SO}_4$  at 304 K are represented in Figure 8(A–C) and the data are summarized in Table IV. the data reveals that; the first oxidation

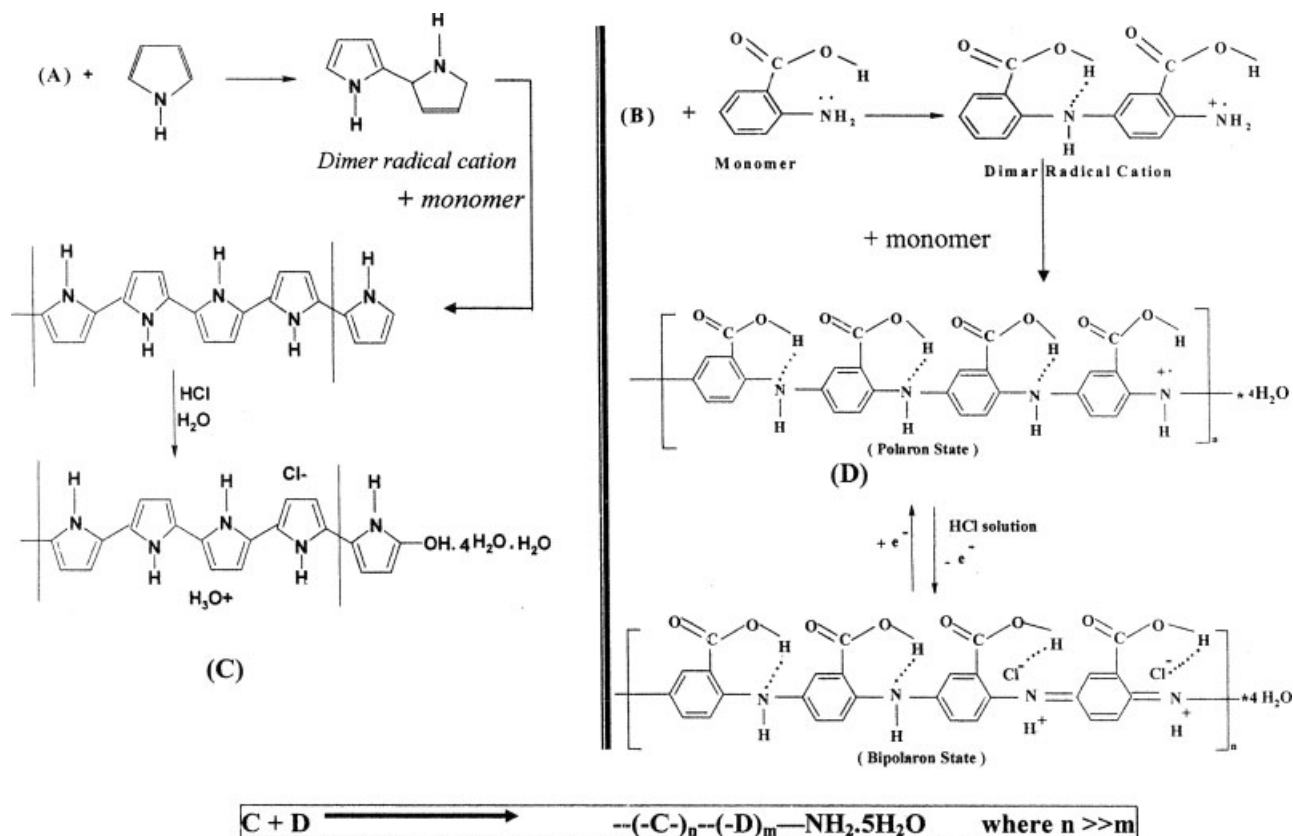
peaks (I) at  $-280$  mV in case of 2-aminobenzoic acid and at  $-400$  mV in case of the binary mixture of *o*-aminobenzoic acid and pyrrole are attributed to the removal of electron from nitrogen atom from *o*-aminobenzoic acid monomer to form radical cation in both cases which react with another molecule of *o*-aminobenzoic acid monomer to form dimer radical cation and so on to form semiquinone radical cation (polaron state).<sup>35</sup> The second oxidation peak (II) at  $+970$  mV in case of *o*-aminobenzoic acid is assigned to the oxidation of semiquinone radical cation (polaron state) to quinonimine (bipolaron state),<sup>35</sup> while the only one oxidation peak observed at  $+790$  mV in case of pyrrole is related to the oxidation of pyrrole monomer to form polypyrrole.<sup>46</sup> Therefore, it can be assumed that the second oxidation peak (II) appears at  $1100$  mV in case of the binary mixture in the comonomer in the electropolymerization bath could be attributed to the oxidation of pyrrole to poly pyrrole (cf. Scheme 1), while the third oxidation peak (III) appears at  $1420$  mV in case of the binary mixture in the electropolymerization bath could be attributed to summation of the oxidation of both *o*-aminobenzoic acid polaron state and the one-step oxidation of pyrrole. The oxidation potentials of the binary mixture are shifted to lower values than those of the two single monomers, indicating that a mixture of both monomers is oxidized more easily than in case of the two separate monomers.

The cathodic span of the reverse scan of the binary monomer mixture does not include any cathodic



**Scheme 1** Formation of radical cations of the two monomers.





Scheme 2 Propagation and formation of the block copolymer.

peak as that appearing in case *o*-aminobenzoic acid (cf. Fig. 8). But current starts to increase forming a reactive anodic peak (IV), indicating the partial removal of the deposited copolymer film from the surface as a result of degradation process and consequently radical cation formation at this potential.

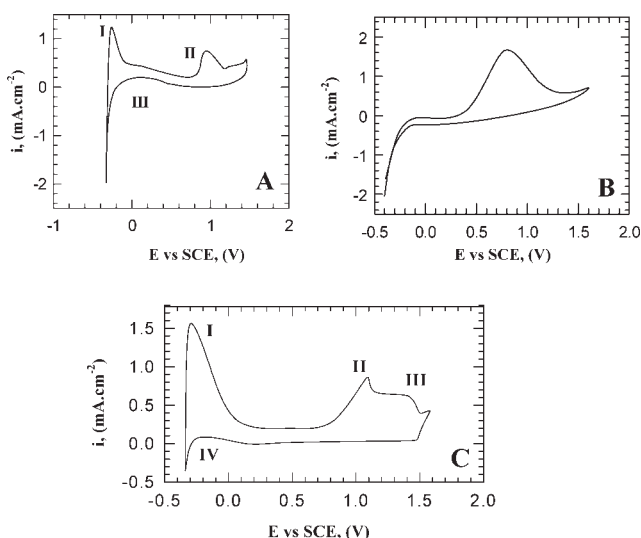


**Figure 8** Cyclic voltammograms curves of Pt in 1M HCl aqueous solution with scan rate  $25 \text{ mVs}^{-1}$  in the presence of (A) *O*-aminobenzoic acid, (B) Pyrrole, and (C) Comonomer.

This indicates that the amount of *o*-aminobenzoic acid segments in the copolymer chains is small in comparison with pyrrole, which is in a good agreement with the data obtained in Figure 7.

### Surface morphology

Homogenous, smooth, black, and well-adhering copolymer films were electrodeposited on platinum surface in most conditions. The surface morphology of the obtained P(OABA-*co*-Py) copolymer and the two homopolymers are examined by scanning electron microscopy and X-ray diffraction analysis. The data shows that,

A. The electropolymerized OABA<sup>35</sup> is crystalline with tubular or fibrillar elongated crystals [cf.

**TABLE IV**  
Cyclic Voltammetry Data for the Electropolymerization of POABA, PPy and P(OABA-*co*-Py) Samples

Monomer name	Anodic oxidation peak potentials (mV vs. SCE)		
	First peak	Second peak	Third peak
<i>O</i> -aminobenzoic acid	-280	+970	-
Pyrrole	+790	-	-
Binary mixture P(OABA- <i>co</i> -Py)	-400	1100	1420

Figs. 9(A) and 10(A)] with two peaks at  $2\theta$  angle equal to 20.841 and 23.007.

- B. The electropolymerized Py<sup>46</sup> is tubular or fibrillar elongated crystals [cf. Figs. 9(B) and 10(B)].
- C. The copolymer is crystalline with tubular or fibrillar elongated structure [cf. Figs. 9(C) and 10(C)] with two peaks at  $2\theta$  angle equal to 20.9 and 23.2.

### CONCLUSIONS

The initial rate of the electrocopolymerization reaction of a binary mixture of *o*-aminobenzoic acid pyr-

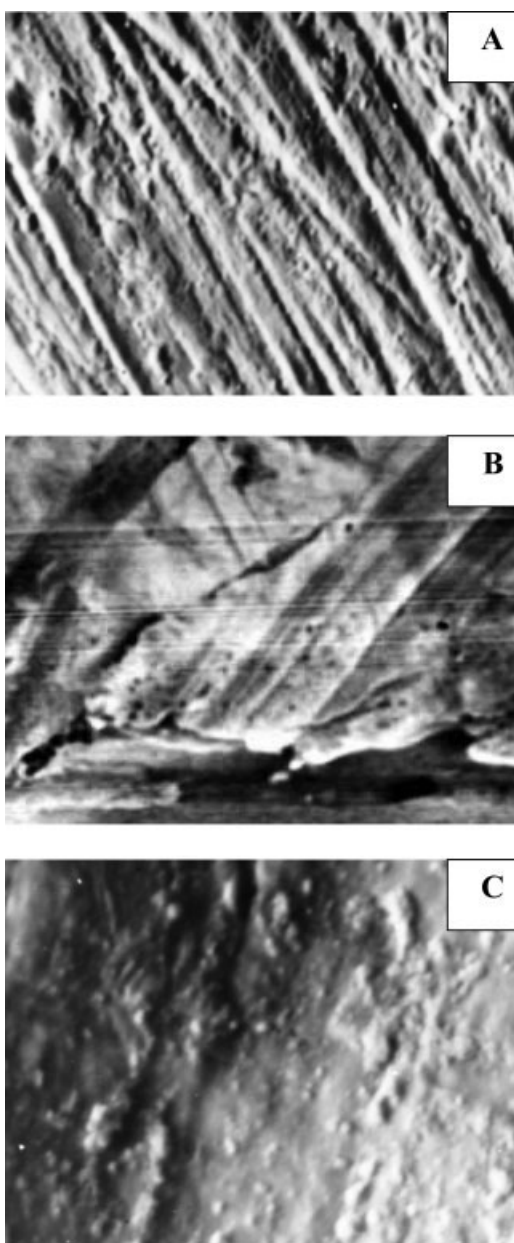


**Figure 9** The picture of scanning electron microscope. A) Poly *o*-aminobenzoic acid. (B) Poly Pyrrole. (C) Copolymer.

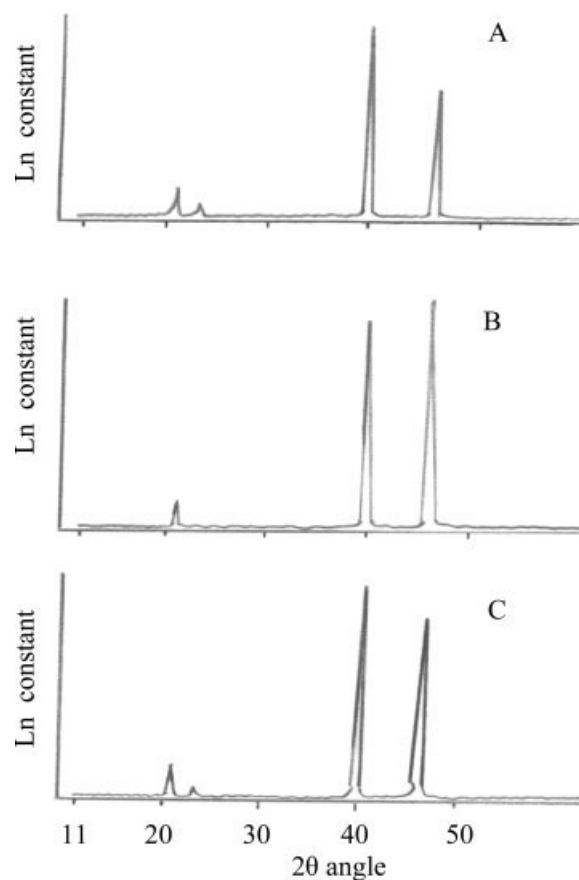


**Figure 10** X-ray diffraction pattern of two homopolymers and copolymer. (A) Poly *o*-aminobenzoic acid. (B) Poly Pyrrole. (C) Copolymer.

role (1 : 1M ratio) on platinum surface is relatively low. The fraction of the dissolved product strongly depends on temperature, monomer and acid concentrations.

The order of the electrocopolymerization reaction is 1.02, 1.44, and 2.00 with respect to current density, hydrochloric acid, and monomer concentration, respectively.

The apparent activation energy of the obtained P(OABA-*co*-Py) copolymer ( $E_a$ ) is 87.75 kJ/mol.

The monomer reactivity ratios, which were calculated according to Fineman-Röss method,  $r_1$  is 1.58, while  $r_2$  is 0.14 and the copolymer structure is a block structure and more rich in pyrrole units.

The oxidation potentials of the binary mixture are shifted to lower values than that of the two separated monomers.

The surface morphology of the obtained copolymer is intermediate between the morphology of the two homopolymers, which is crystalline with tubular or fibrillar elongated structure.

### References

1. Kobayashi, T.; Yoneyama, H.; Tamura H. J Electroanal Chem 1984, 161, 419.

2. Kitani, A.; Kaya, M.; Sasaki, K. *J Electrochem Soc* 1986, 133, 1069.
3. MacDiarmid, A. G.; Yang, L. S.; Hung, W. S.; Humphray, B. D. *Synth Met* 1987, 18, 393.
4. Girard, F.; Ye, S.; Laperriere, G.; Belanger, D. *J Electroanal Chem* 1992, 334, 35.
5. Ye, S.; Girard, F.; Belanger, D. *J Phys Chem* 1993, 97, 12373.
6. Ye, S.; Belanger, D. *J Electrochem Soc* 1994, 141, 149.
7. Nakajima, T.; Kawagoe, T. *Synth Met* 1989, 28C, 629.
8. Geniès, E. G.; Lipkowski, M.; Santier, C.; Viel, E. *Synth Met* 1987, 18, 631.
9. Gottesfeld, S.; Redondo, A.; Feldberg, S. W. *J Electrochem Soc* 1987, 134, 271.
10. Nguyen, M. T.; Deo, L. H. *J Electrochem Soc* 1989, 136, 2131.
11. Paul, E. W.; Ricco, A. J.; Wrighton, M. S. *J Phys Chem* 1985, 89, 1441.
12. Chao, S.; Wrighton, M. S. *J Am Chem Soc* 1987, 109, 6627.
13. Dhaw, S. K.; Trivedi, D. C. *Polym Int* 1991, 25, 55.
14. Joseph, J.; Trivedi, D. C. *J Bull Electrochem* 1992, 22, 563.
15. Thanachasai, S.; Rokutanazono, S.; Yoshida, S.; Watanabe, T. *Anal Sci* 2002, 18, 773.
16. Garcia, M. A. V.; Blanco, B. T.; Ivaska, A. *J Electrochim Acta* 1998, 43, 3533.
17. Nagoaka, T.; Kakuma, K.; Fujimoto, M.; Nakao, H.; Yano, J.; Ogura, K. *J Electroanal Chem* 1994, 369, 315.
18. Anglopoulos, M. *IBM J Res Dev* 2001, 45, 57.
19. Sathiyarayanan, S. K.; Dhawan, S.; Trivedi, D. C.; Balakrishnan, K. *Corr Sci* 1992, 33, 1934.
20. Sazou, D.; Georgolios, C. *J Electroanal Chem* 1997, 429, 81.
21. Troch-Nagels, G.; Winand, R.; Weymeersch, A.; Renard, L. *J Appl Electrochem* 1992, 22, 756.
22. Bernard, M. C.; Joiret, S.; Hugot-LeGoff, A.; Phong, P. V. *J Electrochem Soc* 2001, 148, 12.
23. Brusic, V.; Anglopoulos, M.; Graham, T. *J Electrochem Soc* 1997, 144, 436.
24. Su, W.; Iroch, J. O. *Synth Met* 1998, 95, 159.
25. Dimitra, S. *Synth Met* 2001, 118, 133.
26. Camalet, J. L.; Lacroix, J. C.; Aeiyaich, S.; Chame-Ching, K.; Lacaze, P. C. *Synth Met* 1998, 93, 133.
27. Kinlen, P. G.; Ding, Y.; Silverman, D. C. *Corrosion* 2002, 58, 490.
28. Lu, W. K.; Elsenbaumer, R. L.; Wessling, B. *Synth Met* 1995, 71, 2136.
29. Geniès, E. M.; Boyle, A.; Tapkowisky, M.; Tsivantis, C. *Synth Met* 1990, 36, 139.
30. Cao, Y.; Smith, P.; Heeger, A. *Synth Met* 1992, 48, 91.
31. Yan, H.; Wang, H. J.; Adisasmit, S.; Toshima, N. *Bull Chem Soc Jpn* 1996, 69, 2395.
32. Toshima, N.; Yan, H.; Gotoh, Y.; Ishiwatari, M. *Chem Lett* 1994, 3, 2229.
33. Chan, H. S. O.; Ng, S. C.; Sim, W. S.; Tan, K. L.; Tan, B. T. G. *Macromolecules* 1992, 25, 6029.
34. Thiemann, C.; Brett, C. M. A. *Synth Met* 2001, 123, 1.
35. Sayyah, S. M.; Abd El-Rehim, S. S.; El-Rabiey, M. M.; Azooz, R. E. *Int J Polym Mater* 2006, 55, 37.
36. Yue, J.; Epstein, A. L. *J Am Chem Soc* 1990, 112, 2800.
37. Schneider, O.; Schwitzgebel, G. *Synth Met* 1993, 55, 1046.
38. Diaz, A. F.; Castillo, J. I.; Logan, J. A.; Lee, W. Y. *J Electroanal Chem* 1981, 129, 115.
39. Kanazawa, K. K.; Diaz, A. F.; Krounbi, M. T.; Street, G. B. *Synth Met* 1981, 4, 119.
40. Street, G. B.; Lindsey, S. E.; Nazzal, A. I.; Wynne, K. J. *Mol Cryst Liquid Cryst* 1985, 118, 137.
41. Diaz, A. F.; Hall, B. *IBM J Res Dev* 1983, 27, 342.
42. Munstedt, H.; Naarman, H.; Kohler, G. *Mol Cryst Liquid Cryst* 1985, 118, 129.
43. Cvetko, B. F.; Brungs, M. P.; Burford, R.; Skyllas-Kazacos, M. P. *J Mater Sci* 1988, 23, 2102.
44. Sun, B.; Jones, J. J.; Burfoed, R. P.; Skyllas-Kazacos, M. *J Mater Sci* 1989, 24, 4024.
45. Rhee, H. W.; Jeon, E. J.; Kim, J. S.; Kim, C. Y. *Synth Met* 1989, 28, 605.
46. Sayyah, S. M.; Abdel-Rehim, S. S.; El-Deeb, M. M. *J Appl Polym Sci* 2003, 90, 1783.
47. Sayyah, S. M.; Abdel-Rehim, S. S.; El-Deeb, M. M. *Int J Polym Mater* 2004, 1, 53.
48. Sayyah, S. M.; Abdel-Rehim, S. S.; El-Deeb, M. M. *J Appl Polym Sci* 2004, 94, 941.
49. Sayyah, S. M.; Abdel-Rehim, S. S.; Ibrahim, M. A.; Kamal, S. M. *Int J Polym Mater* 2007, 56, 663.
50. Silverstein, R. M.; Bassler, C. G.; Morill, T. C. *Spectroscopic Identification of Organic Compounds*; Wiley: New York, 1974.
51. Fineman, M.; Röss, S. D. *J Polym Sci* 1950, 5, 250.